Heterometallic Niobium Complexes Containing the "CpNb" Unit. X-ray Crystal Structures of CpNbCl₂(μ-SEt)₂NiCp and CpNb(PhCCPh)(μ-SPrʲ)₂Mo(CO)₄

Simon Woodward[†] and M. David Curtis[*,‡]

Willard H. Dow Chemical Laboratory, University of Michigan, Ann Arbor, Michigan 48109

Arnold L. Rheingold[§] and Brian S. Haggerty

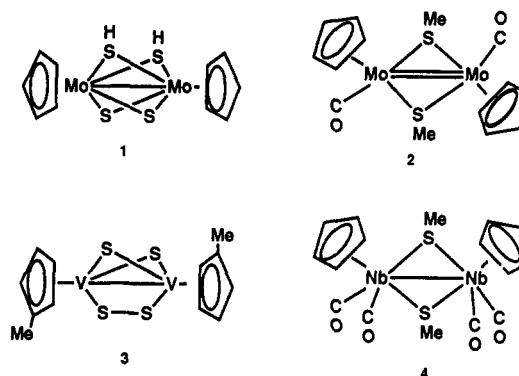*Department of Chemistry, University of Delaware, Newark, Delaware 19716*

Reaction of Cp₂Nb₂Cl₂(μ-Cl₂)(CO)₄ with Cp₂Ni₂(μ-SEt)₂ affords paramagnetic CpNbCl₂(μ-SEt)₂NiCp: ⟨g⟩ = 2.004, A = 129 G; space group = P2₁/c, a = 7.466 (1) Å, b = 28.427 (5) Å, c = 8.620 (2) Å, β = 104.81 (1)°. Addition of LiSPrʲ to CpNbCl₂PhCCPh results in formation of CpNb(SPrʲ)₂(PhCCPh). Reaction of the thiolate complex with Mo(MeCN)₃(CO)₃ and CO (1 equiv) yields CpNb(PhCCPh)(μ-SPrʲ)₂Mo(CO)₄: space group = P2₁/c, a = 16.091 (3) Å, b = 21.186 (5) Å, c = 17.551 (4) Å, β = 90.16 (2)°. However, complex reactivity results on addition of HgCl₂ or Co₂(CO)₈ in the same CpNb(SPrʲ)₂PhCCPh precursor. EHMO analysis of the bonding in CpNbCl₂(μ-SEt₂)NiCp shows the odd electron is localized on the Nb atom, but a substantial Nb–Ni bond exists. The effects of the bridging ligands on the metal–metal overlap populations are described.
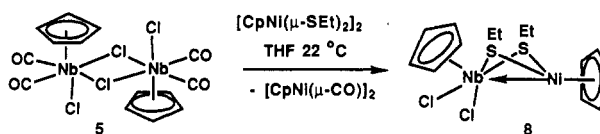
Introduction

For most of the transition metals, examples of heterodinuclear and cluster complexes containing the CpM (Cp = η⁵-C₅H₅, or related derivatives) abound.[1] For the vanadium triad, however, only a few complexes, CpVCo₃-(CO)₉,[2] [CpNb(CO)₃(μ-H)MLₙ]⁻ (M = Cr, Mo, W; L = CO) anions,[3] Cp₄Cr₃MS₄ (M = V, Nb),[4] and Cp₂V₂S₄MₙLₙ (M = Fe, Co, Ir, Ni, Pt; L = CO, NO, PPh₃, Cp) species,[5] are known. Some of these species are only partially characterized. While many heterometallic complexes containing a bis(cyclopentadienyl)–group-5 metal unit (Cp₂M) have been isolated and structurally characterized,[1,6] the related monocyclopentadienyl chemistry remains quite underdeveloped. Recently, we[7] and others[8] have had considerable success in preparing sulfur-containing heterometallic clusters derived from the molybdenum species 1 and 2 (Scheme I).

Such clusters are useful catalyst precursors for certain hydrotreating and CO reduction processes.[9] We sought to extend this chemistry to niobium and tantalum. One major problem with this approach is the inaccessibility of a useful Cp₂M₂Sₙ (M = Nb, Ta) cluster synthon. For example, while the complex Cp′₂V₂S₄ (3) (Cp′ = η⁵-C₅H₄Me) is well-known (Scheme I),[5] niobium and tantalum analogues have yet to be synthesized. Reactions of CpMCl₄ (M = Nb, Ta) with sulfur and selenium transfer reagents lead to mixtures of structurally diverse complexes.[10] Although the syntheses of Cp₂Nb₂(CO)₄(μ-S)ₙ (n = 2, 3) and Cp₂Nb₂(CO)₄(μ-SMe)₂ (4) are reported,[11] their yields are low and their syntheses use CpNb(CO)₄, which in turn requires a very high CO pressure for its preparation.[12] We hoped to circumvent these problems by (i) reaction of appropriate sulfur-containing transition-metal complexes with known group-5 precursors or, alternatively, (ii) by

Scheme I

Scheme II

reacting thiolato (SR) complexes of niobium with unsaturated metal fragments.

† Current address: School of Chemistry, University of Hull, Cottingham Road, Kingston-upon-Hull, HU6 7RX, England. E-mail: sw10%sequent.cc.hull.ac.uk@nsfnet-relay.ac.uk.
‡ E-mail: MDCURTIS@UMICHUM.BITNET.
§ Author to whom enquires regarding the crystal structure data should be made. E-mail: ALQ01424@UDELVM.BITNET.

(1) (a) Roberts, D. A.; Geoffroy, G. L. *Comprehensive Organometallic Chemistry*; Wilkinson, G., Stone, F. G. A. Abel, E., Eds.; Pergamon Press: London, 1982; Vol. 6, Chapter 40 and references within. (b) Stephen, D. W. *Coord. Chem. Rev.* 1989, 95, 41 and references within.
(2) Haustein, H. J.; Schwarzhans, K. E. *Z. Naturforsch., B* 1978, B33, 1108.
(3) Oltmanns, P.; Rehder, D. J. *J. Organomet. Chem.* 1988, 345, 87.
(4) Pasynskii, A. A.; Ermenko, I. L.; Orazsakhator, B.; Kalinnikov, V. T.; Aleksandrov, G. G.; Struchkov, Yu. T. *J. Organomet. Chem.* 1981, 216, 211.
(5) (a) Bolinger, C. M.; Weatherill, T. D.; Rauchfuss, T. B.; Rheingold, A. L.; Day, C. S.; Wilson, S. R. *Inorg. Chem.* 1986, 25, 634. (b) Rauchfuss, T. B.; Weatherill, T. D.; Wilson, S. R.; Zebroski, J. P. *J. Am. Chem. Soc.* 1983, 105, 6508. (c) Bolinger, C. M.; Rauchfuss, T. B.; Wilson, S. R. *J. Am. Chem. Soc.* 1984, 106, 7800.
(6) Darensbourg, M.; Silva, R.; Reibenspies, J.; Prout, C. K. *Organometallics* 1989, 8, 1315.
(7) (a) Curtis, M. D. *Polyhedron* 1987, 6, 759. (b) Curtis, M. D.; Williams, D. P.; Butler, W. M. *Inorg. Chem.* 1988, 27, 2853. (c) Li, P.; Curtis, M. D. *J. Am. Chem. Soc.* 1989, 111, 8279. (d) Li, P.; Curtis, M. D. *Inorg. Chem.* 1990, 29, 1242.

Table I. Crystallographic Data for 8 and 10

	Crystal Parameters	
formula	$C_{14}H_{20}Cl_2NbNiS_2$	$C_{29}H_{29}MoNbO_4S_2$
formula wt	474.94	694.51
space group	$P2_1/c$	$P2_1/c$
cryst syst	monoclinic	monoclinic
a, Å	7.466 (1)	16.091 (3)
b, Å	28.472 (5)	21.186 (5)
c, Å	8.620 (2)	17.551 (4)
β, deg	104.81 (1)	90.16 (2)
V, Å³	1768.8 (6)	5983 (2)
Z	4	8
cryst dimens, mm	0.15 × 0.15 × 0.26	0.20 × 0.36 × 0.40
cryst color	red	red
D(calc), g/cm³	1.784	1.542
μ(Mo Kα), cm⁻¹	22.16	9.31
temp, °C	23	23
T(max)/T(min)	1.28	1.05

	Data Collection	
diffractometer		Nicolet R3m
monochromator		graphite
scan technique		ω
radiation		Mo Kα (λ = 0.710 73 Å)
2θ scan range, deg	4–52	4–50
data collected	$\pm h,+k,+l$	$\pm h,+k,+l$
no. of rflns collected	3794	11217
no. of indpt rflns	2543	10524
no. of obs rflns (F_o > $5\sigma(F_o)$)	2543	6585
std rflns		3 stds/197 rflns
var in stds, %	<1	<1

	Refinement	
$R(F)$, %	3.26	4.43
R(wF), %	3.35	4.59
Δ/σ (final)	0.03	0.03
$\Delta(\rho)$, e/Å³	0.48	0.546
μ_o/μ_v	14.0	10.6
GOF	0.943	1.086

Results and Discussion

Reactions of Niobium Complexes with Sulfur-Containing Organometallics. The reactivity of mono-cyclopentadienyl niobium compounds with sulfur-containing organometallics is quite unpredictable. The interaction of CpNbCl$_4$ or CpNbCl$_2$(PhCCPh) with Li[Fe$_2$-S$_2$(CO)$_6$][13] or related metal sulfide anions leads to complex reduction chemistry.[14] Conversely, no reaction at all is observed between Cp$_2$Nb$_2$Cl$_2$(μ-Cl)$_2$(CO)$_4$ (5) and Fe$_2$S$_2$-(CO)$_6$.[15] However, reaction of 5 and Cp$_2$Ni$_2$(μ-SEt)$_2$ (6) in THF (tetrahydrofuran) proceeds smoothly over 4 h to generate Cp$_2$Ni$_2$(μ-CO)$_2$ (7), detectable by IR spectroscopy, and red, paramagnetic CpNbCl$_2$(μ-SEt)$_2$NiCp (8) (Scheme II). Higher yields of 8 are attained with a longer reaction time (16 h).

Complex 8 is readily separated from hexane-soluble 6 and 7 as deep red plates by virtue of its much lower sol-

(8) (a) Cowans, B. Nourdik, J. Rakowski DuBois, M. *Organometallics* **1983**, *2*, 931. (b) Braunstein, P.; Jud, J. M.; Tiripicchio, A.; Tiripicchio-Camellini, M.; Sappa, E. *Angew. Chem., Int. Ed. Engl.* **1982**, *21*, 307. (c) Braunstein, P. Tiripicchio, A.; Camellini, M.; Sappa, E. *Inorg. Chem.* **1981**, *20*, 3586.

(9) (a) Curtis, M. D.; Penner-Hahn, J. E.; Baralt, O.; McCabe, D. J.; Thompson, L. *Polyhedron* **1988**, *7*, 2411. (b) Thompson, L. T.; Schwank, J.; Curtis, M. D. *J. Am. Inst. Chem. Eng.* **1989**, *35*, 109. (c) Riaz, U.; Curnow, O.; Curtis, M. D. *J. Am. Chem. Soc.* **1991**, *113*, 1416.

(10) Fenske, D. Ohmer, J. Hachgenei, I.; Merzweiler, K. *Angew. Chem., Int. Ed. Engl.* **1988**, *27*, 1277.

(11) Hermann, W. A.; Biersack, H.; Ziegler, M. L.; Balbach, B. *J. Organomet. Chem.* **1981**, *206*, C33.

(12) Hermann, W. A.; Biersack, H. *J. Organomet. Chem.* **1980**, *191*, 397.

(13) Seyferth, D.; Henderson, R. S.; Song, L.-C. *Organometallics* **1982**, *1*, 125.

(14) These reactions typically result in poorly soluble, ill-characterized metal sulfides.

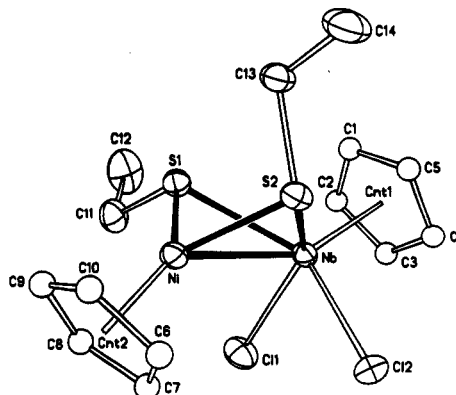(15) Hieber, W.; Gruber, J. Z. *Anorg. Allg. Chem.* **1958**, *296*, 91.

Figure 1. Molecular structure and labeling scheme for CpNbCl$_2$(μ-SEt)$_2$NiCp (8).

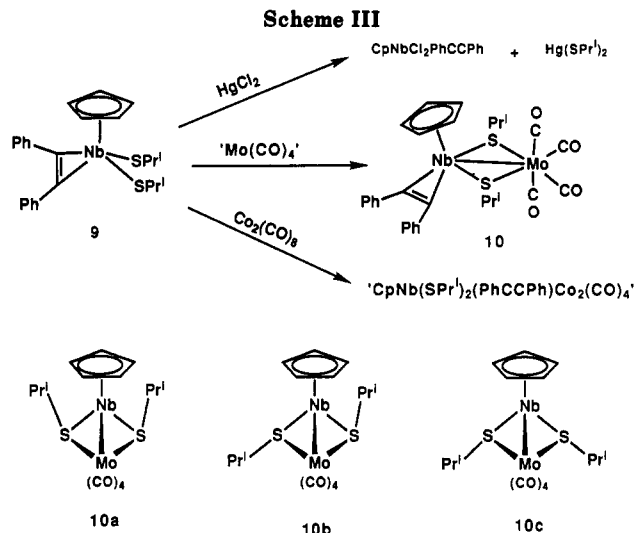**Table II. Atomic Coordinates (×10⁴) and Isotropic Thermal Parameters (Å² × 10³) for 8**

	x	y	z	U^a
Nb	460.1 (5)	3868.2 (1)	4752 (5)	28.2 (1)
Ni	-848.4 (7)	3667.1 (2)	1529.2 (7)	29.4 (2)
S(1)	1745 (2)	3355.3 (4)	2920 (1)	33.4 (4)
S(2)	329 (2)	4366.8 (4)	2303 (2)	33.1 (4)
Cl(1)	-1210 (2)	3179.0 (5)	5415 (2)	48.9 (5)
Cl(2)	-2433 (2)	4304.3 (5)	4626 (2)	47.9 (5)
C(1)	3619 (8)	4001 (4)	6063 (8)	85 (3)
C(2)	2998 (8)	3681 (2)	6974 (7)	62 (2)
C(3)	1711 (9)	3910 (3)	7593 (7)	83 (3)
C(4)	1599 (12)	4362 (3)	7060 (12)	129 (4)
C(5)	2774 (15)	4410 (3)	6079 (10)	134 (5)
C(6)	-3524 (6)	3853 (2)	310 (7)	46 (2)
C(7)	-3620 (6)	3479 (2)	1333 (6)	45 (2)
C(8)	-2651 (7)	3104 (2)	874 (7)	50 (2)
C(9)	-2075 (7)	3240 (2)	-517 (7)	54 (2)
C(10)	-2618 (7)	3703 (2)	-873 (7)	55 (2)
C(11)	1574 (8)	2722 (2)	3251 (7)	49 (2)
C(12)	3396 (9)	2544 (2)	4309 (9)	76 (3)
C(13)	2577 (7)	4410 (2)	1782 (6)	42 (2)
C(14)	3054 (8)	4916 (2)	1615 (9)	70 (3)

^{a} Equivalent isotropic U defined as one-third of the trace of the orthoganalized U_{ij} tensor.

Table III. Selected Bond Lengths (Å) and Angles (deg) for 8

Nb–Ni	2.759 (1)	Nb–S(1)	2.513 (1)
Nb–S(2)	2.524 (1)	Nb–Cl(1)	2.467 (1)
Nb–Cl(2)	2.469 (1)	Nb–C(1)	2.370 (6)
Nb–C(2)	2.384 (5)	Nb–C(3)	2.390 (5)
Nb–C(4)	2.406 (9)	Nb–C(5)	2.378 (9)
Ni–S(1)	2.187 (1)	Ni–S(2)	2.208 (1)
Ni–C(6)	2.074 (4)	Ni–C(7)	2.102 (5)
Ni–C(8)	2.074 (5)	Ni–C(9)	2.144 (6)
Ni–C(10)	2.155 (5)	S(1)–C(11)	1.833 (5)
S(2)–C(13)	1.849 (6)	C(1)–C(2)	1.358 (11)
C(1)–C(5)	1.327 (13)	C(2)–C(3)	1.377 (10)
C(3)–C(4)	1.360 (13)	C(4)–C(5)	1.372 (15)
C(6)–C(7)	1.395 (8)	C(6)–C(10)	1.426 (8)
C(7)–C(8)	1.401 (8)	C(8)–C(9)	1.427 (9)
C(9)–C(10)	1.388 (9)	C(11)–C(12)	1.518 (8)
C(13)–C(14)	1.498 (8)		
Ni–Nb–S(1)	48.8 (1)	S(1)–Nb–S(2)	74.9 (1)
Ni–Nb–S(2)	49.2 (1)	S(1)–Nb–Cl(1)	88.9 (1)
Ni–Nb–Cl(1)	89.9 (1)	S(2)–Nb–Cl(2)	80.5 (1)
Ni–Nb–Cl(2)	88.8 (1)	Cl(1)–Nb–Cl(2)	85.4 (1)
S(2)–Nb–Cl(1)	136.6 (1)	S(1)–Nb–Cl(1)	137.2 (1)
Nb–Ni–S(1)	59.7 (1)	S(1)–Ni–S(2)	88.3 (1)
Nb–Ni–S(2)	59.9 (1)	Nb–S(1)–Ni	71.5 (1)
Nb–S(2)–Ni	71.0 (1)	Ni–S(2)–C(13)	107.6 (2)
Nb–S(1)–C(11)	113.3 (2)	Nb–S(2)–C(13)	113.4 (2)
Nb–S(1)–C(11)	114.8 (2)		

ubility and high degree of crystallinity. Paramagnetic 8 shows a single broad resonance at δ 6.16 in its ^{1}H NMR spectrum and this is attributed to the Me groups of the

Scheme III

Figure 2. Variable-temperature ^{1}H NMR spectra of CpNb-(PhCCPh)(μ-SPr^i)$_2$Mo(CO)$_4$ (10) in the cyclopentadienyl and isopropyl regions at 300.1 MHz in CDCl$_3$.

Figure 3. Molecular structure and labeling scheme for CpNb-(PhCCPh)(μ-SPr^i)$_2$Mo(CO)$_4$ (10).

SEt units. No other signals are detected within 60 ppm of TMS. A CH$_2$Cl$_2$ solution at room temperature shows the expected 10-line ESR multiplet ($\langle g \rangle$ = 2.004, A_{Nb} = 129 G) for a d^1 niobium(IV) complex. At the signal-to-noise level in typical spectra, no coupling to nickel (^{61}Ni, 1.1% abundant, spin = $^3/_2$) is apparent, even in concentrated solutions, suggesting that the odd electron is primarily localized on the Nb center. To help ascertain the nature of any metal–metal interaction in 8, a crystallographic study was undertaken. An ORTEP view of the molecule is presented in Figure 1; data relevant to the structure are collected in Tables I–III. The Nb–Ni distances of 2.759 (1) Å is consistent with the presence of a dative bond and is reminiscent of the Nb–Ni distances (2.77 Å) encountered in the structure of [{Cp$_2$Nb(μ-SMe)$_2$}$_2$Ni][BF$_4$]$_2$.[16] The two Nb–S–Ni angles at 71.0 (1) and 71.5 (1)° are also comparable to those in the dication structure (average Nb–S–Ni = 72.5°).[16] The NbS$_2$Ni ring is puckered; similar geometries are known.[11,17] The Nb–Cl distances (2.549 (1) and 2.467 (1) Å) fall within expected ranges as do the average Nb–C (2.386 (9) Å) and Ni–C (2.110 (6) Å) distances for the cyclopentadienyl rings. The syn/anti arrangement of the SEt groups is probably a crystal packing effect. Conformer interconversion in solution is common for such species.[18]

One might expect 5 to react with other thiolate dimers leading to formation of other new heterometallics, but this is not the case. No reaction of 5 with Cp$_2$Mo$_2$(CO)$_4$(μ-SMe)$_2$, Mn$_2$(CO)$_8$(μ-SMe)$_2$, or Fe$_2$(CO)$_6$(μ-SEt)$_2$ is observed. The formation of 8 is best accounted for as a redox reaction in which the Nb(III) center in 5 is oxidized to niobium(IV), while one of the nickel centers in 6 is reduced to nickel(I). The facile reaction of 5 with 6 is thus attributed to the ease of reduction of 6 with subsequent labilization of the thiolato ligands.

The nickel–niobium complex 8 itself is rather unreactive. Attempted reduction under various conditions (Al/HgCl$_2$/CO, Na/Hg/CO, NaC$_{10}$H$_8$/CO, Na/Hg/PMe$_3$)

leads only to decomposition, as does reaction with MeLi. The compound is also unreactive toward PhCCPh, CO, (Me$_3$Si)$_2$S, PhOH, and atmospheric oxygen. Reaction with excess NO results in the formation of CpNiNO and a highly insoluble, uncharacterized niobium species.

Syntheses via CpNb(SPr^i)$_2$PhCCPh. The complex CpNb(SPr^i)$_2$PhCCPh (9) is readily available by the reaction of known[19] CpNbCl$_2$PhCCPh with LiSPr^i. The complex shows the expected spectroscopic properties. In particular, the ^{13}C NMR chemical shift of the alkyne carbons [δ (CDCl$_3$) 201.6] is indicative of a four-electron alkyne donor.[20] The sulfur lone pairs should allow the complexation of a large range of second metal centers to 9. In practice, however, reactivity is only observed in only a few cases. The reaction of Mo(NCMe)$_3$(CO)$_3$ with 9 in the presence of 1 equiv of CO results in the clean formation of CpNb(PhCCPh)(μ-SPr^i)$_2$Mo(CO)$_4$ (10) in moderate yield (59%) as the sole organometallic product (Scheme III).

The absence of added CO results in a complex mixture of products from which only 10 can be separated by fractional crystallization, albeit in low yield (29%). Complex 10 is fluxional. A room temperature ^{1}H NMR spec-

(16) (a) Douglas, W. E.; Green, M. L. H.; Prout, C. K.; Rees, G. V. *J. Chem. Soc., Chem. Commun.* **1971,** *896.* (b) Prout, K.; Critchley, S. R.; Rees, G. V. *Acta Crystallogr., Sect. B* **1974,** *B30,* 2305.

(17) Benson, I. B.; Killops, S. D.; Know, S. A. R.; Welch, A. J. *J. Chem. Soc., Chem. Commun.* **1980,** 1137.

(18) (a) Collman, J. P.; Hegedus, L. S.; Norton, J. R.; Finke, R. G. *Principles and Applications of Organotransition Metal Chemistry,* 2nd ed.; University Science Books: Mill Valley, CA, 1987; pp 63, 64. (b) Ruffing, C. J.; Rauchfuss, T. B. *Organometallics* **1985,** *4,* 524. (c) Cameron, T. S.; Prout, C. K.; Rees, G. V.; Green, M. L. H.; Joshi, K. K.; Davies, G. R.; Kibourn, B. T. *J. Chem. Soc., Chem. Commun.* **1971,** 14. (d) Douglas, W. E.; Green, M. L. H. *J. Chem. Soc., Dalton Trans.* **1972,** 1796.
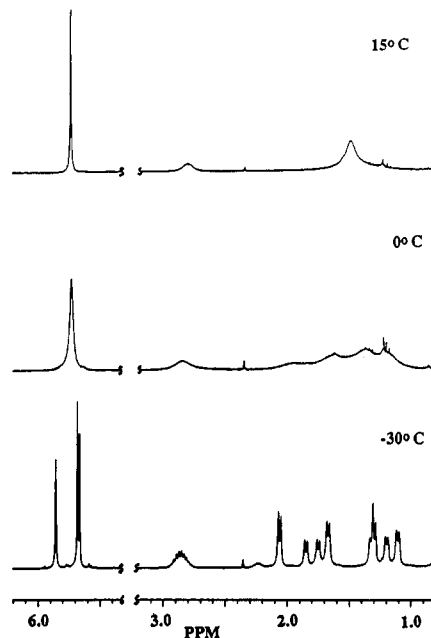
(19) (a) Curtis, M. D.; Real, J. *Organometallics,* **1985,** *4,* 940. (b) Curtis, M. D.; Real, J.; Kwon, D. *Organometallics* **1989,** *8,* 1644.

(20) Templeton, J. L.; Ward, B. C. *J. Am. Chem. Soc.* **1980,** *102,* 3288.

Table IV. Atomic Coordinates (×10⁴) and Isotropic Thermal Parameters (Å² × 10³) for 10

	x	y	z	U^a
Nb	3410.2 (3)	7421.9 (3)	8028.1 (3)	37.5 (2)
Nb'	1607.0 (3)	2577.1 (3)	2603.8 (3)	39.3 (2)
Mo	2278.4 (3)	6391.7 (3)	8564.2 (3)	43.5 (2)
Mo'	2745.1 (3)	1526.4 (3)	3072.6 (4)	44.9 (2)
S(1)	2141 (1)	7043 (1)	7358 (1)	42 (1)
S(2)	3507 (1)	6863 (1)	9264 (1)	47 (1)
S(1')	2856 (1)	2218 (1)	1901 (1)	42 (1)
S(2')	1496 (1)	1944 (1)	3784 (1)	50 (1)
O(1)	678 (3)	5654 (2)	8039 (4)	94 (3)
O(2)	1123 (3)	7461 (2)	9277 (3)	69 (2)
O(3)	3443 (4)	5385 (3)	7735 (4)	106 (3)
O(4)	2010 (4)	5590 (4)	10058 (4)	119 (3)
C(1)	1269 (4)	5934 (3)	8206 (4)	61 (3)
C(2)	1539 (4)	7088 (3)	9031 (4)	48 (2)
C(3)	3026 (5)	5742 (3)	8054 (5)	66 (3)
C(4)	2141 (5)	5887 (4)	9517 (4)	72 (3)
C(5)	2334 (4)	6602 (3)	6453 (4)	57 (3)
C(6)	2170 (5)	7057 (4)	5810 (4)	84 (4)
C(7)	1767 (6)	6034 (4)	6369 (5)	97 (4)
C(8)	4399 (4)	6312 (3)	9387 (5)	67 (3)
C(9)	5101 (5)	6689 (4)	9753 (5)	95 (4)
C(10)	4159 (6)	5764 (4)	9891 (6)	118 (5)
C(11)	4092 (4)	7429 (4)	6789 (4)	74 (3)
C(12)	4322 (4)	7990 (4)	7180 (4)	70 (3)
C(13)	4806 (4)	7806 (4)	7802 (4)	69 (3)
C(14)	4858 (5)	7148 (5)	7787 (5)	79 (4)
C(15)	4417 (5)	6927 (4)	7179 (5)	80 (3)
C(16)	2731 (4)	8268 (3)	8151 (4)	41 (2)
C(17)	3301 (4)	8249 (3)	8687 (4)	43 (2)
C(21)	4262 (3)	8450 (2)	9772 (3)	61 (3)
C(22)	4576	8849	10335	69 (3)
C(23)	4275	9464	10401	87 (4)
C(24)	3658	9679	9905	124 (5)
C(25)	3344	9280	9342	86 (4)
C(26)	3645	8665	9276	44 (2)
C(31)	1444 (3)	8898 (3)	8344 (3)	79 (3)
C(32)	867	9343	8092	96 (4)
C(33)	932	9597	7362	92 (4)
C(34)	1576	9406	6883	147 (6)
C(35)	2153	8961	7135	119 (5)
C(36)	2088	8707	7865	47 (2)
O(3')	1603 (4)	531 (3)	2206 (4)	90 (2)
O(1')	4353 (3)	830 (2)	2488 (4)	109 (3)
O(2')	3905 (3)	2596 (2)	3804 (3)	65 (2)
O(4')	3012 (4)	707 (3)	4543 (4)	122 (3)
C(3')	2022 (4)	884 (3)	2526 (4)	59 (3)
C(1')	3770 (4)	1098 (3)	2686 (5)	74 (3)
C(2')	3484 (4)	2217 (3)	3557 (4)	48 (2)
C(4')	2905 (5)	999 (4)	3993 (5)	72 (3)
C(5')	2639 (4)	1799 (3)	990 (4)	61 (3)
C(6')	2745 (5)	2276 (4)	362 (4)	89 (4)
C(7')	3235 (6)	1251 (4)	874 (5)	105 (4)
C(8')	607 (4)	1376 (3)	3829 (5)	67 (3)
C(10')	875 (5)	780 (4)	4253 (5)	94 (4)
C(9')	−94 (5)	1707 (4)	4258 (6)	104 (4)
C(14')	135 (5)	2400 (6)	2388 (6)	98 (5)
C(15')	533 (6)	2142 (5)	1785 (7)	99 (5)
C(11')	903 (5)	2603 (5)	1380 (5)	89 (4)
C(12')	742 (5)	3182 (4)	1747 (5)	83 (3)
C(13')	246 (5)	3034 (5)	2385 (5)	79 (4)
C(16')	2309 (4)	3408 (3)	2789 (4)	44 (2)
C(17')	1762 (4)	3358 (3)	3335 (4)	44 (2)
C(31')	3531 (3)	4121 (2)	2998 (2)	62 (3)
C(32')	4116	4551	2728	80 (4)
C(33')	4141	4699	1954	82 (4)
C(34')	3582	4417	1450	85 (4)
C(35')	2997	3986	1720	73 (3)
C(36')	2972	3838	2494	49 (2)
C(25')	1757 (3)	4324 (2)	4140 (3)	74 (3)
C(24')	1438	4673	4746	101 (4)
C(23')	788	4430	5181	79 (3)
C(22')	456	3839	5009	71 (3)
C(21')	776	3490	4402	65 (3)
C(26')	1426	3733	3968	48 (2)

^{a} Equivalent isotropic U defined as one-third of the trace of the orthogonalized U_{ij} tensor.

Table V. Selected Bond Distances (Å) and Angles (deg) for One Independent Molecule of 10^a

Nb–Mo	2.996 (1)	Nb–C(16)	2.111 (6)
Nb–S(1)	2.487 (2)	Nb–C(17)	2.107 (6)
Nb–S(2)	2.476 (2)	Mo–S(1)	2.537 (2)
Mo–C(1)	1.992 (7)	Mo–S(2)	2.530 (2)
Mo–C(4)	2.009 (8)	S(1)–C(5)	1.868 (7)
Mo–C(2)	2.065 (6)	S(2)–C(8)	1.862 (7)
Mo–C(3)	2.037 (7)	C(16)–C(17)	1.312 (9)
C(16)–C(36)	1.478 (8)	C(17)–C(26)	1.466 (8)
C–O(av)	1.15 (2)	Nb–C(av)	2.43 (1)
CpC–C(av)	1.39 (2)		
Mo–Nb–S(1)	54.2 (1)	S(1)–Nb–S(2)	108.0 (1)
Mo–Nb–S(2)	54.1 (1)	S(1)–Mo–S(2)	104.9 (1)
Mo–Nb–C(16)	105.8 (2)	S(1)–Nb–C(16)	84.1 (2)
Mo–Nb–C(17)	112.4 (2)	S(2)–Nb–C(17)	85.5 (2)
Nb–Mo–S(1)	52.6 (1)	S(2)–Nb–C(16)	110.4 (2)
Nb–Mo–S(2)	52.4 (1)	S(1)–Nb–C(17)	117.3 (2)
S(1)–Mo–C(1)	86.1 (2)	S(2)–Mo–C(1)	168.7 (2)
S(1)–Mo–C(2)	83.9 (2)	S(2)–Mo–C(2)	88.6 (2)
S(1)–Mo–C(3)	92.9 (2)	S(2)–Mo–C(3)	91.1 (2)
S(1)–Mo–C(4)	168.7 (2)	S(2)–Mo–C(4)	84.1 (2)
Nb–Mo–C(1)	138.7 (2)	C(1)–Mo–C(2)	90.1 (3)
Nb–Mo–C(2)	87.5 (2)	C(1)–Mo–C(3)	90.8 (3)
Nb–Mo–C(3)	89.6 (2)	C(1)–Mo–C(4)	84.7 (3)
Nb–Mo–C(4)	136.5 (2)	C(2)–Mo–C(3)	176.6 (3)
Nb–S(1)–Mo	73.2 (1)	C(2)-Mo–C(4)	89.5 (3)
Nb–S(2)–Mo	73.5 (1)	C(3)–Mo–C(4)	93.8 (3)
Mo–S(1)–C(5)	115.0 (2)	Nb–S(1)–C(5)	115.1 (2)
Mo–S(2)–C(8)	114.2 (2)	Nb–S(2)–C(8)	116.6 (3)
Nb–C(16)–C(36)	149.6 (4)	C(16)–C(17)–C26	138.5 (5)
Nb–C(17)–C(26)	148.8 (4)	C(17)–C(16)–C36	138.5 (6)
Mo–C–O(av)	177.0 (1)		

^{a} Bond distance and angles of the second independent molecule are within 3σ of corresponding values reported here.

trum in CDCl₃ shows a single Cp signal, while the isopropyl resonances are very broad (Figure 2). On cooling, three distinct isomers are detected at −30 °C. This fluxionality is due to interconversion of the isomers 10a–c; such isomerism is very common in bridging thiolate complexes.[6,18] The presence of three isomers is also detected in the low-temperature ¹³C NMR spectrum (75.5 MHz) of 10. For the mixture 10a–c 14 CO and alkyne carbon signals are predicted. Only 13 are observed; however, one of these at δ 208.5 is appreciably broadened and this is probably due to an accidental superposition.

For comparison with the nickel–niobium structure 8, the crystal structure of 10 was solved. Two independent molecules of 10 are present. An ORTEP view of one of the independent molecules is shown in Figure 3. The crystal, refinement, coordinate, and geometrical data are presented in Tables I, IV, and V. A Nb–Mo bond of 2.996 (1) Å is seen for both molecules. Unlike the one in 8, the NbS₂Mo torus is almost planar, while the Nb–S–Mo angles 73.2 (1), 73.4 (1), 73.5 (1), and 73.6 (1)° are slightly larger than those seen in 8. The molybdenum is essentially octahedral with the two axial carbonyls bent back very slightly [C(2)–Mo–C(3) 176.6 (3)°; C(2')–Mo–C(3') 175.9 (3)°]. All attempts (thermal, photolytic, chemical) to labilize a CO from 10 and hence generate a niobium–molybdenum double bond were unsuccessful, as were attempts to react it with PhCCPh.

Reaction of HgCl₂ with CpNb(SPrⁱ)₂PhCCPh (9) results in a mixture of products that is difficult to separate. However, of interest is the reformation of CpNbCl₂PhCCPh with concomitant formation of Hg-(SPrⁱ)₂ (Scheme III). Such reactivity is an interesting example of the hard–soft acid–base concept.[21] Cobalt

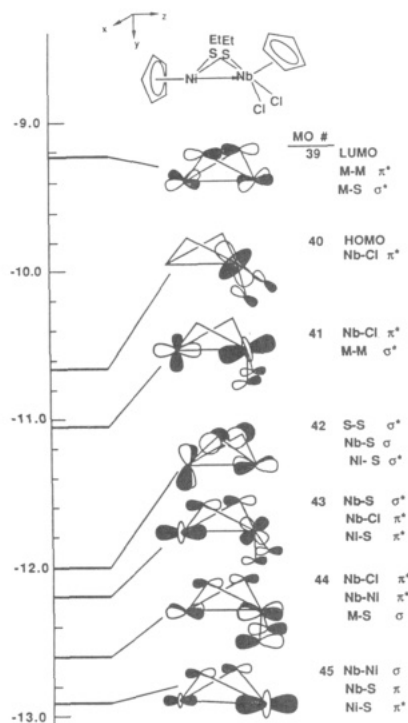(21) Huheey, J. E. *Inorganic Chemistry*, 3rd ed.; Harper International: Cambridge, 1983; pp 312–322.

Figure 4. Schematic frontier molecular orbitals for CpNbCl$_2$-(μ-SH)$_2$NiCp.

carbonyl reacts with **9** in toluene cleanly forming a single product by IR and ^{1}H NMR spectroscopy. The product is thermolabile both in solution and the solid state at room temperature, making its full characterization difficult. The available spectroscopic data (IR, ^{1}H NMR, and FAB mass spectroscopy) suggest that the compound is "CpNb-(SPr^i)$_2$PhCCPhCo$_2$(CO)$_4$" (Scheme III). The highest m/e peak in the FAB mass spectrum corresponds to the addition of O + H$^+$ to the formula given, but it is believed that the oxygen and proton were transferred from the sulfolane matrix since the IR spectrum does not suggest the presence of S=O functionality or oxidized cobalt (normal ν_{CO}). Recrystallization at low temperatures leads, in the best cases, to small black plates that are poor X-ray crystallographic subjects. Attempted trapping reactions of CpNb(SPr^i)$_2$PhCCPhCo$_2$(CO)$_4$ with PPh$_3$ or PMe$_3$ led only to decomposition.

EHMO Analysis of the Bonding in 8. Because the Ni–Nb distance (2.76 Å) in **8** suggests the presence of a substantial Ni–Nb interaction or bond, whereas the ESR spectrum shows the odd electron is primarily localized on Nb and has little interaction with the Ni atom, an EHMO calculation on the idealized molecule, CpNi(μ-SH)$_2$NbCl$_2$Cp (**8i**), was performed. The idealized structure, **8i**, was given interatomic distances and angles as found in the crystal structure of **8** or averages of these values so as to give **8i** C_s symmetry. Some of the results of the calculation are shown in Figure 4.

In accordance with the conclusion drawn from the observed hyperfine splitting, the calculated HOMO containing the odd electron is 70% localized on the Nb atom, 26% on the two Cl atoms, and only 1.5% on the Ni atom. One would therefore not expect detectable Ni hyperfine splitting. The observed Nb hyperfine coupling, 128 G, is somewhat smaller than that observed in some related Nb(IV) complexes[22] (ca. 150–160 G), which suggests that the delocalization of the odd electron onto the ligands in **8** is greater than usual. The HOMO corresponds ap-
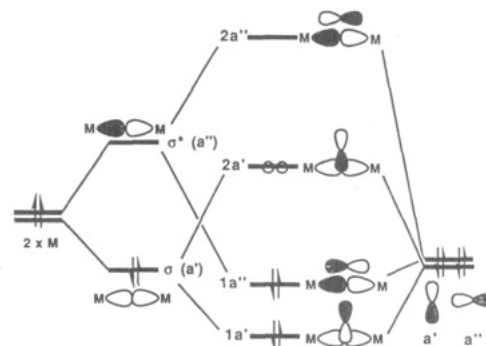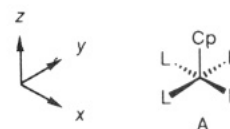

Figure 5. Schematic interaction for bridging atom p-orbitals and metal–metal MO's.

proximately to a "d$_{xy}$ orbital" in the coordinate system for a four-legged piano stool shown in A. In other words, the

energies of the frontier d-orbitals on Nb are primarily determined by familiar ligand field effects. The lowest energy orbital of the formally Nb(IV) ion points between the ligands and is nonbonding in the σ-framework. This orbital has the correct symmetry to π-bond with chloride ligands, however, and the HOMO indeed shows Nb–Cl π*-character as expected (the π-bonding orbitals are at much lower energy). There is essentially no involvement of sulfur or nickel orbitals in the HOMO. The sulfur π-orbitals are in the wrong orientation to π-bond as a result of the SR group conformation necessary to form the bridge bonds to Ni.[23]

Although the HOMO has little contribution from Ni, there is a substantial Ni–Nb interaction. The Mulliken overlap population (MOP) for the Ni–Nb bond is calculated to be 0.20. While not large, this value is respectable for a metal–metal bond. For comparison, the MOPs for the Ni–S, Nb–S, and Nb–Cl bonds are 0.28, 0.57, and 0.55, respectively. It is well recognized that it is difficult to draw conclusions concerning the strength or even the presence of metal–metal bonds in the presence of bridging ligands. The origin of the difficulty can be understood by reference to Figure 5.

Figure 5 shows the simplified case of one group, X, bridging a homonuclear metal–metal bond. Assume one orbital from each metal is used to form M–M σ- and σ*-bonds of symmetry a′ and a″. Further assume the bridging ligand, X, has atomic or group orbitals of a′ and a″ symmetry (as do bridging sulfides or thiolates). These may correspond to p-orbitals perpendicular and parallel to the M–M axis, respectively. The AOs of X may make bonding and antibonding combinations with the σ- and σ*-orbitals as shown in Figure 5. The 1a′ MO is both M–M and M–X bonding; but the 1a″ orbital is M–M antibonding and M–X bonding. The bridging ligand causes occupation of M–M σ*-orbitals, thus lowering the overall MOP of the metal–metal bond. Depending on the number of electrons involved, the 2a′ orbital (Figure 5) may also be occupied. In this case, orbitals that are M–M bonding but M–X antibonding are occupied.

This simple picture gets more complicated as the number of bridging ligands and number of orbitals on the metal atoms available for bonding increases, i.e., as π, π*, δ, and

(22) Curtis, M. D.; Real, J. *Inorg. Chem.* **1988**, *27*, 3176.

(23) For interesting structural effects caused by SR group orientations, see: Curnow, O. J.; Kampf, J.; Curtis, M. D. *Inorg. Chem.* **1991**, *30*, 4043.

$\delta*$ bonds become possible in addition to σ- and $\sigma*$-combinations. Nevertheless, the general principle remains that M–X bonding can cause population of M–M antibonding orbitals and M–M bonding orbitals may be M–X antibonding. The MOs diagrammed in Figure 4 show several examples of these effects.

For heteronuclear M–M' bonds, the situation gets even more complex: an MO may be M–X bonding and M'–X antibonding and vice versa. Such a situation may arise when one metal–X interaction dominates due to better energy matching or better overlap. The magnitude, and even the sign, of the X–M and X–M' d_{z^2} overlap intergrals, $\langle p_z(X)|z^2(M \text{ or } M')\rangle$, will depend strongly on the geometry of the M–X–M' triangle. In the case of 8, these overlap integrals are dominated by p-orbital interaction with the "belly band" portion of the d_{z^2}-orbital and the values for the $\langle$sulfur $p_z|$metal $d_{z^2}\rangle$ integrals are shown below. Thus, in an M–M bonding MO formed by the overlap of two d_{z^2}-orbitals, admixture of a p_z-orbital of the bridging sulfide will give a bonding Nb–S and an antibonding Ni–S interaction as exemplified by MO 45 in Figure 4. The MOPs between atoms are the sums of all these types of interactions, and, in the case of bridged M–M bonds, the mix of the various interactions described above spreads the contributions to the M–M bond over so many MOs that it often becomes impossible to pick out one or two that adequately describe the M–M or M–X bond. Such is the case here.

$$S(p_z|Ni\text{-}dz^2)= +0.038 \qquad S(p_z|Nb\text{-}dz^2)= -0.055$$

The MOPs are usually taken to be a measure of the degree of bonding. Thus, one would conclude from the relative values of the Nb–S and Ni–S MOPs, 0.57 and 0.28, that the Nb–S bond is stronger than the Ni–S bond. Is the bridging thiolato sulfur "closer", in a relative sense, to Nb than to Ni, allowing for the different inherent bond lengths? The Ni–S and Nb–S bond lengths are 2.20 and 2.52 Å, respectively. The sum of the covalent radii[24] of Ni (1.21 Å) and S (1.01 Å) is 2.23 Å, which compares very well with the observed value. Thus the Ni–S bond distance appears normal. One-half of the Nb–Nb distance (about 3.06 Å) in CpNb(II) dimers[25] may be a good value for the covalent radius of Nb in these complexes, or r(Nb) = 1.53 Å. Thus the "predicted" Nb–S and Nb–Ni distances are 2.54 and 2.74 Å, respectively. These values are very close to the observed distances of 2.52 and 2.76 Å. Hence, the Nb–S and Nb–Ni distances also appear to be "normal".

Thus, the very large difference in the Nb–S and Ni–S MOPs is not reflected by a shorter Nb–S or a longer Ni–S bond. On an orbital by orbital comparison, Nb–S overlap integrals are 1.5–10 times larger than the corresponding Ni–S integrals. Since the overlap populations are the sums of terms, e.g., $n_k c_{ki} c_{kj} S_{ij}$, a larger overlap integral (S_{ij}) will tend to give larger MOPs. Therefore, comparing MOPs of heteronuclear bonds to assess relative bonding interactions may give very misleading results as the present example demonstrates.

Experimental Section

All manipulations were carried out under nitrogen atmospheres by using glovebox or Schlenk techniques. Solvents were distilled just prior to use from an appropriate drying agent. The compounds [CpNbCl(μ-Cl)(CO)$_2$]$_2$ (5),[19] [CpNi(μ-SEt)]$_2$ (6),[26] and

CpNbCl$_2$(PhCCPh)[19] are available through literature procedures. Infrared spectra were recorded on a Nicolet 5DB instrument. Proton NMR (300.1 MHz) and ^{13}C NMR (75.5 MHz) spectra were recorded on a Bruker AM-300 spectrometer. Mass spectra were obtained on a VG-70-250S machine using either EI or FAB ionization modes. Elemental analyses were performed by either Galbraith Laboratories Inc. or by the University of Michigan analytical service.

CpNbCl$_2$(μ-SEt)$_2$NiCp (8). Tetrahydrofuran (THF) (250 mL) was added by cannula to a mixture of solid [CpNbCl(μ-Cl)(CO)$_2$]$_2$ (5) (1.00 g, 1.75 mmol) and [CpNi(μ-SEt)]$_2$ (6) (1.30 g, 3.51 mmol). The reaction was stirred (16 h) at ambient temperature, during which time it became dark red and IR spectra indicated the formation of [CpNi(μ-CO)]$_2$ (7). The solvent was removed under vacuum. The residue was extracted with CH$_2$Cl$_2$/toluene (1:1) (3 × 75 mL) and the extracts filtered through a Celite pad. The solution was concentrated to about 30 mL and layered and hexane (60 mL). On standing at room temperature (2 h) red microcrystals formed. Removal of the mother liquors, washing with hexane, and drying yielded 8, 0.89 g (53%). The mother liquors were evaporated to dryness and the residue triturated with copious quantities of hexane to dissolve [CpNi(μ-CO)]$_2$ (7) and unreacted 6. The residue was recrystallized from CH$_2$Cl$_2$/hexane to yield more 8, 0.32 g (18%). Total yield of red microcrystalline CpNbCl$_2$(μ-SEt)$_2$NiCp (8) was 1.21 g (71%). ^{1}H NMR (CDCl$_3$, 25 °C) δ 6.16 (s, br, possible Me); ESR (CH$_2$Cl$_2$, 25 °C) $\langle g \rangle$ = 2.004, A_{Nb} = 129 G; MS (EI), m/z 473 [M$^+$ NiCl$_2$ pattern]. Anal. Calcd for C$_{14}$H$_{20}$Cl$_2$NbNiS$_2$: C, 35.41; H, 4.24; C, 14.93; S, 13.50. Found: C, 35.27; H, 4.19; Cl, 14.99; S, 14.00.

Reaction of CpNbCl$_2$(μ-SEt)$_2$NiCp (8) with NO. Nitric oxide gas was blubbled through a solution of 8 (0.10 g, 0.21 mmol) in THF (20 mL) for 10 min. The reaction changed color from red to orange/yellow and an IR spectrum [ν_{NO} (THF) 1811 s cm^{-1}] indicated the formation of CpNiNO. The volatiles were removed under vacuum, giving a red THF solution of CpNiNO with identical properties to an authentic sample. The yellow residue remaining was extracted with THF (3 × 10 mL), the extracts were filtered through Celite, and the solvent was removed to give a yellow powder. All attempts to characterize this paramagnetic product were foiled by its poor crystallinity and solubility.

CpNb(SPr^i)$_2$(PhCCPh) (9). A suspension of Pr^{i}SLi (prepared from Pr^{i}SH (0.5 mL, 5.28 mmol) and MeLi (3.0 mL, 1.75 M, 5.25 mmol)) in toluene (20 mL) was added to CpNbCl$_2$(PhCCPh) (1.09 g, 2.68 mmol) in toluene (100 mL) at 0 °C. The reaction mixture became yellow/orange immediately but was stirred (1 h) at 0 °C during which time NaCl formation was noted. The reaction mixture was filtered through a Celite pad with a toluene wash and the solvent removed under vacuum. The resulting orange oil was extracted with hexane (3 × 50 mL), and the extracts were filtered through Celite. The solution was concentrated until crystallization was just apparent. Storage at −10 °C afforded CpNb(SPr^i)$_2$(PhCCPh) (9) as an orange solid, 0.70 g (58 %), of sufficient purity for subsequent reactions. The analytical sample was recrystallized from hexane, from which complex 9 forms orange microcrystals. ^{1}H NMR (CDCl$_3$, 25 °C) δ 1.11 (d, J = 7 Hz, 6 H, Me), 1.31 (d, J = 7 Hz, 6 H, Me) 3.34 (septet, J = 7 Hz, 2 H, CH), 6.04 (s, 5 H, Cp), 7.29–7.36 (m, 2 H, Ph-p), 7.42–7.49 (m, 4 H, Ph-m), 7.63–7.68 (m, 4 H, Ph-o); ^{13}C NMR (CDCl$_3$, 25 °C) δ 26.0 (Me), 26.7 (Me), 44.4 (CH), 106.2 (Cp), 128.0 (Ph-p), 128.3 (Ph-m), 128.7 (Ph-o), 139.3 (Ph-i), 201.6 (alkyne C); MS (EI), m/z 486 [M$^+$]. Anal. Calcd for C$_{25}$H$_{29}$NbS$_2$: C, 61.72; H, 6.01. Found: C, 61.68; H, 6.00.

CpNb(PhCCPh)(μ-SPr^i)$_2$Mo(CO)$_4$ (10). Solid Mo(MeCN)$_3$(CO)$_3$ (0.25 g, 0.83 mmol) was added to a solution of CpNb(SPr^i)$_2$(PhCCPh) (9) (0.40 g, 0.82 mmol) in toluene (100 mL) and the reaction vessel was isolated from the rest of the Schlenk line. Using a syringe, CO gas (20 mL, 0.81 mmol) was promptly added via a rubber septum. The reaction was stirred at ambient temperature (3 h), during which time the Mo(MeCN)$_3$(CO)$_3$ dissolved and a deep red solution formed. Infrared spectroscopy showed that 10 was the only carbonyl compound present. The solvent was removed and the residue extracted with hexane/toluene (4:1) (3 × 40 mL). The extracts were filtered

(24) Huheey, J. E. *Inorganic Chemistry, Principles of Structure and Reactivity*, 2nd ed.; Harper and Row: New York, 1978.

(25) Kwon, D.; Real, J.; Curtis, M. D.; Rheingold, A.; Haggerty, B. S. *Organometallics* 1991, *10*, 143.

(26) Schropp, W. K. *J. Inorg. Nucl. Chem.* 1962, *24*, 1688.

through a Celite pad and concentrated to a minimal volume, and hexane (3 mL) was added. After 1 h, removal of the mother liquors and drying afforded CpNb(PhCCPh)(μ-SPr^i)$_2$Mo(CO)$_4$ (10) as red microcrystals, 0.33 g (59%). In the absence of added CO a complex mixture of products formed, from which only 10 could be isolated as red crystals (29%) by repeated fractional crystallization from toluene/hexane. IR ν_{CO} (toluene) 2031 s, 1945 s, 1925 s cm^{-1}; ^{1}H NMR (CDCl$_3$, -30 °C) δ 1.10 (d, J = 6 Hz, 6 H, 2 Me), 1.19 (d, J = 6 Hz, 3 H, Me), 1.26 (d, J = 6 Hz, 6 H, 2 Me), 1.32 (d, J = 6 Hz, 3 H, Me), 1.66 (d, J = 6 Hz, 6 H, 2 Me), 1.74 (d, J = 6 Hz, 3 H, Me), 1.84 (d, J = 6 Hz, 3 H, Me), 2.05 (d, J = 6 Hz, 6 H, 2 Me), 2.23 (m, 2 H, 2CH), 2.87 (m, 4 H, 4CH), 5.66 (s, 5 H, Cp), 5.67 (s, 5 H, Cp), 5.85 (s, 5 H, Cp) (ratio of Cp peaks 2:4:3), 7.12–7.15 (m, 4 H, Ph-*o*), 7.19–7.21 (m, 4 H, Ph-*o*), 7.25–7.45 (m, 18 H, Ph-*m*+*p*), 7.67–7.70 (m, 4 H, Ph-*o*); ^{13}C NMR (CDCl$_3$, -30 °C) δ 27.0, 27.4, 28.0 (sh), 28.1, 28.2, 28.7, 29.0, 29.2 (all Me), 45.1, 47.2, 48.7, 49.7 (all CH), 100.2, 101.9, 103.1 (all Cp), 125.5, 126.6, 127.1, 127.5, 127.9, 128.0 (m), 129.2 (all Ph), 137.7, 140.4, 142.6 (all Ph-*i*), 193.7, 199.6, 201.4, 202.3, 204.1, 204.4, 204.8, 206.8, 208.5 (br) (all CO or alkyne C), 219.0, 219.5, 219.8, 220.4 (all CO); MS (EI), *m*/*z* 668 [(M – CO)$^+$]. Anal. Calcd for C$_{29}$H$_{29}$MoNbO$_4$S$_2$: C, 50.15; H, 4.21. Found: C, 50.53; H, 4.36.

Reaction of HgCl$_2$ with CpNb(SPr^i)$_2$(PhCCPh) (9). Solid HgCl$_2$ (0.13 g, 0.47 mmol) was added to a solution of CpNb(SPr^i)$_2$(PhCCPh) (9) (0.23 g, 0.47 mmol) in toluene (30 mL). The yellow solution rapidly darkened to orange while the HgCl$_2$ dissolved over the course of 1 h. The mixture was filtered through Celite with a toluene wash and the solvent removed. The oily red residue was extracted with hexane, yielding impure Hg(SPr^i)$_2$, identified by comparison with an authentic sample. A ^{1}H NMR spectrum showed the remaining red material to be a mixture of three products CpNbCl$_2$(PhCCPh) [δ (C$_6$D$_6$) 5.73, Cp] and two unidentified species [δ (C$_6$D$_6$) 5.85, Cp; 6.01, Cp]. Repeated fractional crystallization gave only small amounts of impure CpNbCl$_2$(PhCCPh), 0.013 g (7%).

Reaction of Co$_2$(CO)$_8$ with CpNb(SPr^i)$_2$(PhCCPh) (9). Solid Co$_2$(CO)$_8$ (0.19 g, 0.56 mmol) was added to 9 (0.25 g, 0.51 mmol) dissolved in toluene (30 mL). The mixture was stirred for 2.5 h at room temperature, during which time it became very dark and IR spectroscopy showed the formation of a new species [ν_{CO} (toluene) 2028 s, 1977 s cm^{-1}]. The solvent was removed. Extraction with toluene and filtration through Celite gave a dark solution, which was concentrated to ca. 4 mL, cooled to 0 °C, and layered with an equal volume of hexane. After 1 h the mother liquors were syringed off to give black crystals, 0.26 g. This compound is thermolabile. Decomposition at room temperature precluded elemental analysis. Attempted trapping reactions of the complex with PPh$_3$ or PMe$_3$ afforded no isolabile products. Yield 70%. IR ν_{CO} (toluene) 2028 s, 1977 s cm^{-1}; ^{1}H NMR (C$_6$D$_6$, 25 °C) δ 0.97 (d, J = 6 Hz, 3 H, Me), 1.04 (d, J = 6 Hz, 3 H, Me), 1.16 (d, J = 6 Hz, 3 H, Me), 1.38 (d, J = 6 Hz, 3 H, Me), 1.81 (septet, J = 6 Hz, 1 H, CH), 1.93 (septet, J = 6 Hz, 1 H, CH),

5.58 (s, 5 H, Cp), 6.46–6.53 (m, 2 H, Ph), 6.68–6.95 (m, 6 H, Ph), 7.00–7.15 (m, 2 H, Ph); MS (FAB, sulfolane matrix) 733 [P$^+$], 705, 677, 648, 621 [(P – *n*CO)$^+$] (*n* = 1, 2, 3, 4), 578, 535 [P – 4CO – *n*Pr^i)$^+$] [*n* – 1, 2).

X-ray Structure Determinations for CpNbCl$_2$(μ-SEt)$_2$NiCp (8) and CpNb(PhCCPh)(μ-SPr^i)$_2$Mo(CO)$_4$ (10). X-ray Data Collection for 8 and 10. Crystal, data collection, and refinement parameters are given in Table I. Crystals of 8 were grown by slow diffusion of hexane into a CH$_2$Cl$_2$ solution of the complex. Crystals of 10 were obtained by slow cooling of a toluene/hexane mixture to 0 °C. Data were collected at ambient temperature on crystals mounted on glass fibers with epoxy cement. The unit-cell parameters were obtained from the least-squares fit of the angular settings of 25 reflections (20° $\leq$ 2θ $\leq$ 30°). Preliminary photographic characterization showed that both 8 and 10 to be monoclinic and of space group *P*2$_1$/*c*. Empirical absorption corrections were applied to the data sets for both crystals.

Structural Solution and Refinement for 8 and 10. Both 8 and 10 were solved by direct methods. All non-hydrogen atoms were refined anisotropically, but all hydrogen atoms were included as idealized isotropic contributions. The phenyl rings of 10 were constrained to be rigid hexagons. For 10, the crystallographic asymmetric unit consisted of two independent but chemically indentical molecules. All computer programs are contained in the SHELXTL program library (version 5.1, Nicolet Corp., Madison, WI).

EHMO calculations were performed with R. Hoffmann's program ICONS with the weighted H_{ij} option.[27] Atomic parameters have been described previously.[19b] The molecule 8i was given the endo–endo configuration for the SH groups, d(S–H) = 1.33 Å. Other relevant distances (where different from the X-ray structure) are Nb–Cp(centroid), 2.10; Nb–C(Cp), 2.43; Ni–Cp(centroid), 1.74; Ni–C(Cp), 2.125; Nb–Cl, 2.47; Nb–S, 2.51; and Ni–S, 2.20. The dihedral angle between the NbNiS planes was 108°, and the Cl–Nb–Cl angle was 90.0°.

Supplementary Material Available: Tables of bond distances and angles, anisotropic thermal parameters, and hydrogen atom coordinates for 8 and 10 (12 pages). Ordering information is given on any current masthead page.

OM920028M

(27) Ammeter, J. H.; Burgi, H.-B.; Thibault, J. C.; Hoffmann, R. *J. Am. Chem. Soc.* **1978**, *100*, 3686.